FIBEROPTIC SMART SENSING OF COMPONENT DEFORMATIONS IN ADAPTIVE WINGS

D. Betz, M. N. Trutzel, L. Staudigel, W. Martin*, O. Krumpholz
DaimlerChrysler AG, Research and Technology
Optical Interconnects and Optical Sensors (FT2/HV), 89081 Ulm, Germany
***Structural Materials (FT4/W), 81663 Munich, Germany**
daniel.betz@daimlerchrysler.com

Keywords: *Bragg grating sensors, sensor reliability, thermal / mechanical stability, adaptive wing*

Abstract

This paper presents research activities focusing on the use of fiberoptic Bragg grating sensors in a broad range of modern transportation systems in the aerospace, automotive, and railway industries. The application of Bragg grating sensors in airplane wings and especially in future adaptive wings is illustrated. A challenge associated with using Bragg grating sensors in real-world applications is that an extremely high thermal and mechanical reliability of up to 10-30 years is required for the sensors. Therefore, this work deals with experimental results concerning the mechanical and thermal performance of fiberoptic Bragg grating sensors. Special focus will be put on the reliability of draw-tower fabricated gratings. In addition, the impact of the fiber coating on the sensor sensitivity will be generally discussed. We will report on a field test performed at DASA Airbus on the surface of a newly developed wing consisting of a carbon fiber-reinforced material. The results of the field test clearly show the functionality of the fiberoptic sensor system based on Bragg gratings.

Introduction

One example for the application of fiberoptic Bragg grating sensors is deployment in the wing of an airplane, especially in an adaptive wing, which is in the pipeline. The technical objective in the development of an adaptive wing is to find structure-dynamic solutions which fully deploy the aerodynamic potential in passenger and transport aircraft to increase lift and to reduce air drag. This results in enhanced performance, improved fuel economy, increased payload and lower operating costs [1].

A significant contribution to reducing aerodynamic drag and, hence, to cutting fuel consumption constitutes the development of a variable-geometry wing with a profile that can be adjusted optimally to flight conditions via a control loop sensor/processor/actuator. In order to measure the wing profile at a given time, the adaptive wing needs ideally positioned sensors which provide the input signals for the control loop [2].

Because of their small size, light weight, intrinsic nature, and excellent multiplexing capabilities, fiberoptic Bragg grating sensors seem to be the best candidate for constructing large strain sensor networks which can also be integrated into fiber-composite structures. Recent work in our laboratory has shown that, applying fiber grating sensors produced using a single excimer laser pulse at the draw-tower, a fracture stress distribution >4 GPa is achieved with nearly no difference to a reference distribution without gratings. So, draw-tower gratings are very promising strain and temperature sensor candidates even with respect to reliability aspects. We consequently focus on the results of our work on the reliability of these draw-tower gratings.

1 Bragg Grating Sensors

A fiberoptic Bragg grating (FBG) is a permanent, periodic perturbation of the refractive index (Figure 1) which is laterally exposed into the core of an optical fiber, extending over a limited length of the fiber [3].

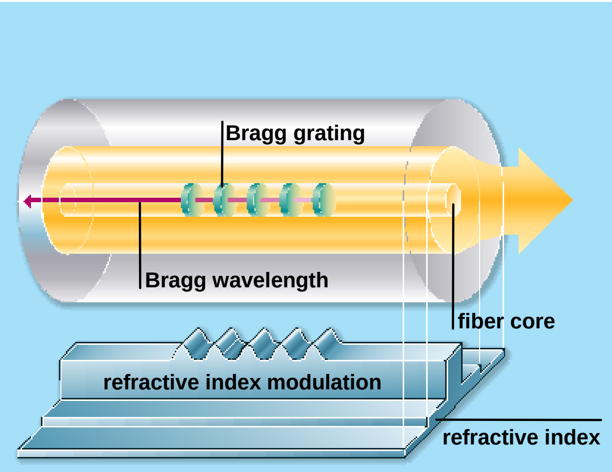

Figure 1: Fiberoptic Bragg Grating

The grating is characterized by its period, amplitude, and length (usually 1-20 mm). Such a periodic structure acts as a filter for light traveling along the fiber line. It has the property of reflecting light in a predetermined range of wavelength centered around a peak wavelength value. This value, the Bragg wavelength λ_B, is given as follows:

$$\lambda_B = 2 \cdot \bar{n}_{eff} \cdot \Lambda \qquad (1)$$

Λ is the grating period and $\bar{n}_{eff}$ is the mean effective refractive index in the grating region. External forces such as strain, pressure or a temperature change lead to changes in the grating period and in the effective refractive index. Consequently, the wavelength of the light reflected from the grating varies. The relative shift of the Bragg wavelength for an applied strain along the fiber axes ε_z and a temperature change ΔT is, in a first approximation, given as follows:

$$\frac{\Delta\lambda_B}{\lambda_B} = C_\varepsilon \cdot \varepsilon_z + C_T \cdot \Delta T \qquad (2)$$

C_ε and C_T are material constants usually determined from calibration experiments. Typical values for the relative shift of the Bragg wavelength are ~10 pm/K for the temperature sensitivity and ~1.2 pm/με (1 με≡1 μm/m) for the strain sensitivity in the 1.5 μm wavelength region [3, 4].

2 Fabrication of FBGs

For the production of FBGs, an optical fiber is illuminated with ultraviolet (UV) light. The effect of photosensitivity in germanium-doped silicate glasses is used to obtain a UV light-induced change in the refractive index. The amplitude of the index change depends on a variety of parameters:

1. The wavelength of the light used for inscribing the FBG.
2. The intensity of the UV beam.
3. The total energy dose of the beam.
4. The composition of the glass.
5. The treatment of the fiber before UV illumination.
6. The achievable contrast in the structuring process.

See [3] for an in-depth description of the physical context. It is essential to note that all the parameters also have a critical influence on the mechanical and thermal properties of the gratings, a fact that is currently not fully understood.

There are a number of possible fabrication processes [3]. The periodic exposure may be performed either using two-beam interferometry or by near-field holography through an optical transmission phase mask.

A major concern associated with using Bragg grating sensors in real-world applications is that an extremely high thermal and mechanical reliability of up to 10-30 years is required for the sensors. In the standard grating fabrication process, the coating of the fiber has to be stripped off and the grating is then written inside the bare fiber. Finally, the fiber has to be recoated to ensure that it may be handled and for mechanical protection. This process dramatically decreases the mechanical strength of the fiber and increases fabrication costs [5,6]. To avoid problems associated with the decoating and recoating processes, two – basically different – approaches have arisen. The first technique is of major interest. It allows the inscription of the gratings on-line, during fiber-drawing, by a single laser shot [7]. This technique can currently only be handled by Naval Research (USA) [8], IPHT e.V. Jena (Germany) [9] and NASA (USA) [10]. The other technique focuses on the use of UV-transparent fiber coatings, so that the gratings can be inscribed through the coating [11]. However, to date these coatings are not suitable for deployment in strain applications because the material properties are insufficient for the high demands placed on the coating material.

3 Aspects of Fiber Coating

A number of requirements which the coating has to fulfill in order to be used in fiber sensor applications have been set.

1. There should be high adhesion for the coating on the glass-surface, as environmental forces have to be transferred through the coating. As has been shown in push-out experiments, not only are there great differences in the adhesion between polyimide and acrylate coatings but also disparities between two differing polyimide coatings [12]. Moreover, the coating has to transfer the forces without creeping or slipping.
2. The fiber strength has to be warranted even in humid and harsh environments. The coating also affects the stress corrosion of the optical fiber and the optical attenuation (microbending losses).
3. The required temperature range extends the range of telecom applications. Typical coatings for standard telecom applications can be used between –50 to +85 °C. This range is not sufficient for many sensor applications e.g. in aerospace systems. For example, the curing temperature for modern fiber-reinforced composites which can be used for the structural integration of FBGs, is 200 °C and therefore much higher than the specified maximum temperature for telecom applications.
4. The material properties of the coating (Young's modulus, thermal expansion coefficient, coating thickness) have to be chosen individually for each application. For example, when gluing FBG sensors on the surface of structures, we computed the strain transfer as a function of coating parameters with a finite-element (FE) model [13]. Our results showed that it is crucial to make sure that the modulus of the fiber coating is sufficiently high to transfer the strain being measured into the core of the fiber sensor over a glued length, which is comparable to the processing by electrical strain gauges. Another example for the application of FBGs is their structural integration into modern fiber-reinforced composites. We were able to show that by the use of an appropriate coating, stress concentrations in the fiber-matrix interface can be minimized and the sensor response affected [14].
5. The change in the material properties due to temperature change and humidity has a negative impact on the sensor function. In Figure 2, the temperature response of a FBG with and without an acrylate coating is illustrated. It is evident that there is a strong non-linearity in the temperature response of the FBG with acrylate coating at negative temperatures. We calculated the thermal stress produced within the fiber by the coating. Taking into account the change in Young‘s modulus due to the glass transition of the coating, we found a substantial agreement between theory and practice [15].

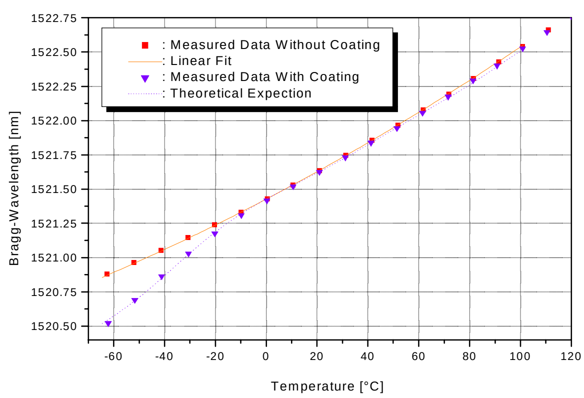

Figure 2: Temperature Response of a FBG with and Without Acrylate Coating

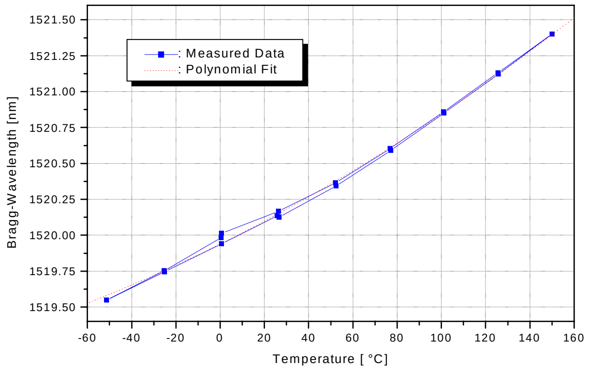

Figure 3: Hysteresis in the Temperature Response of a FBG with Polyimide Coating

Figure 3 shows the hysteresis in the temperature response of a FBG with polyimide coating. To obtain this result, we did three temperature loops from 25° C to -50 C, then to 150° C and back to 25° C. Hysteresis was observed in the temperature range between 0° C and 50 C. The reason for this is believed to be the water absorption of the coating. We noticed the hysteresis in the temperature response of some FBGs from different suppliers with distinct polyimide coatings, whereas some FBGs did not show this behavior at all. Such effects as hysteresis and non-linearities in the temperature response due to the coating have to be avoided for FBGs in sensor applications.

Table 1 shows the properties of some selected coating materials. The data was obtained using [16, 17, 18]. Compared to the above-described requirements set for coatings in strain-sensing applications, polyimide and ORMOCER® are the materials with the greatest advantages. ORMOCER® (**or**ganically **mo**dified **cer**amics) is a novel polymer-based material which was developed by the Fraunhofer Institute for Silicate Research (ISC) in Wuerzburg (Germany) at the beginning of the nineties. Compared to polyimide, it has a higher adhesion on glass and – as a main advantage – it can be UV-cured. This is a valuable benefit for the on-line fabrication of Bragg gratings on the draw-tower. Also, recent work in our laboratory has shown that, using Bragg gratings with a special ORMOCER® coating, the effect of water absorption and the corresponding hysteresis in the temperature response can be dramatically decreased.

	Acrylate	***Polyimide***	***Metal (Aluminum)***	***Carbon (glassy-amorph)***	***ORMOCER®***
Temperature range of use [in °C]	-50 to +85	-100 to350	to 400	to 600	-60 to ~200
Adhesion on glass	low	average to high	average to high	high	high
Curing	UV	thermal (UV?)	specific process	specific process	UV
Young's Modulus [MPa]	1 to 2000	1000 to 6000	~70000	~30000	1 to 4000
Temperature dependency of Young's Modulus in the range from –50 to +100 °C	high	low	low	low	low
Coating thickness [µm]	20-60	5-20	a few µm	<1	10-30
Absorption of water	average	average to low	no	no	depends
Influence on micro-bending losses	low	average to low	high	high	average to low
Splicing performance	excellent	good	poor	poor	good

Table 1: Properties of Selected Coating Materials

4. Mechanical Characterization

A systematic investigation of the mechanical reliability of off-line fabricated Bragg gratings with acrylate coatings has been performed by Limberger et al. [19, 20]. Results showed that the fabrication of high-strength Bragg gratings (off-line) is feasible, at least over short periods, using appropriate decoating and recoating techniques and using a continuous-wave UV laser to inscribe the gratings. However, the application of these techniques is time consuming and costly, and it has not yet been proven for other types of fiber coatings (e.g. polyimide coatings) often used in sensor applications. Also, a UV pulse laser is commonly used in the standard fabrication process for Bragg gratings and no special care is taken to obtain mechanical resistance. To better illustrate the problem associated with the standard fiber fabrication process, we compare the Weibull distribution of on-line fabricated gratings (fibers with and without gratings from the IPHT in Jena, Germany) with off-line fabricated gratings in Figure 4. The mechanical characterization of the gratings was performed using a conventional translation test apparatus. The fracture strength of the fibers was measured under dynamic loading conditions (axial tension) and exploited according to IEC 793-1-3 [21]. We tested 15 specimens at a strain rate of 10 mm/min. The measured quantities for each sample were the force and the time. As usual, to evaluate data from mechanical experiments, the cumulative fracture probability F is computed as a function of the dynamic shape and scaling parameters m and σ_0 and the stress σ [22].

$$F = 1 - \exp\left\{ -\left(\frac{\sigma}{\sigma_0} \right)^m \right\} \qquad (3)$$

Hardly any difference can be seen between the Weibull distribution of on-line fabricated gratings and the distribution of the fibers without gratings. On the contrary, there is a great difference between on-line fabricated gratings and the off-line fabricated gratings. The median breaking strength σ_0 is 5.18 GPa for the on-line fabricated gratings, 5.25 GPa for the reference fibers and only 1.49 GPa for the off-line fabricated gratings. Furthermore, the width of the distribution for the off-line fabricated gratings is much greater than is the case for the others. The median breaking strength and the width of the distribution determine not only the maximum usable strain range but also the lifetime of the sensors at considerably lower strain levels. Hence, on-line fabricated Bragg grating sensors should be deployed in applications where higher strain levels are expected and/or a long lifetime is required.

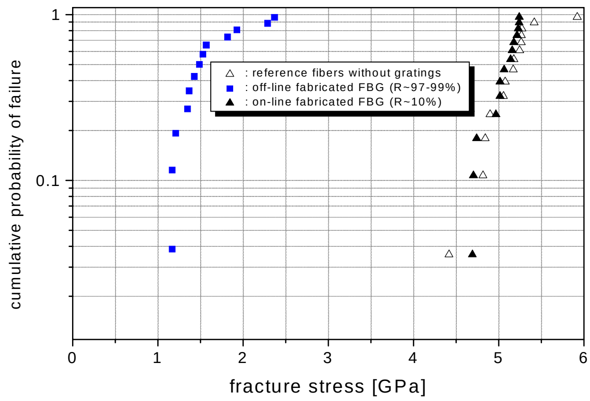

Figure 4: Typical Fracture Stress Distribution for Off-Line and On-Line Fabricated FBGS.

So far we have not specified the fabrication of the off-line gratings in greater detail. But, as noted above, the mechanical strength of the grating is a function of a large number of process parameters. Many of these parameters are correlated with the UV source and the UV illumination, e.g. the total energy dose, single pulse energy, pulse frequency. To be sure to be able to differentiate between the individual parameters necessitates a decoating and recoating process which does not affect the mechanical strength. For this purpose, the University (TU) of Dresden, Germany, provided us with gratings where the decoating and recoating problem was solved by using a thermal decoating technique. Again, for the analysis of the mechanical strength of the gratings, a two-parameter Weibull distribution is assumed. Figure 5 shows the cumulative fracture probability as a function of the fracture stress.

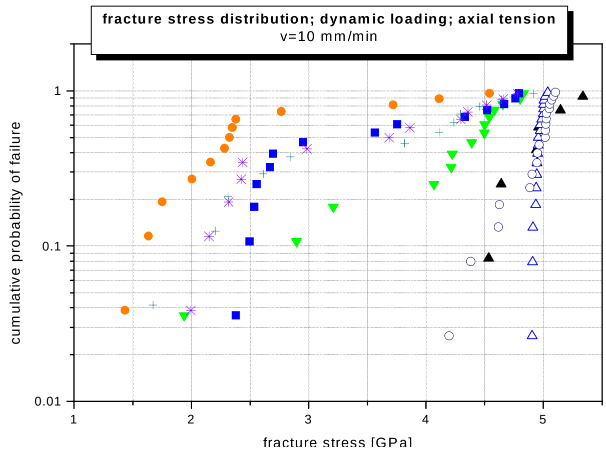

Figure 5: Fracture Stress Distribution; Influence of UV Illumination

samples TU Dresden
- ▲ thermal decoated + recoated
- ▼ therm.dec.+ rec. + illuminated [400mJ/1'/50Hz; i.e. 1200J]
- ■ therm.dec.+ rec. + illuminated [360mJ/1'/10Hz; i.e. 216 J]
- + therm.dec.+ rec. + grating [150mJ/5'/50Hz; i.e. 2250J / R~86%]
- ● therm.dec.+ rec. + grating [450mJ/2'/50Hz; i.e. 2700J / R~64%]
- ★ therm.dec.+ rec. + illuminated [400mJ/5'/10Hz; i.e. 1200J]

samples IPHT Jena
- △ reference fiber
- ○ on-line fabricated gratings (R~2-3%)

As the figure shows, the UV illumination of the fibers has a strong influence on their mechanical strength. The curves of the non-illuminated, simply decoated and recoated fibers show that their mechanical strength can be compared to the mechanical strength of the reference fibers, at least over a certain time and with a considerable technical effort. A higher pulse frequency seems to have a positive influence on the mechanical strength, whereas a high single-pulse energy dramatically decreases the mechanical strength. On the other hand, there is no unambiguous performance in the variation of the total energy dose.

Corresponding to the results of Limberger et al. [20,21], it follows that, for the fabrication of Bragg gratings, the total energy dose and the single-pulse energy have to be as low as possible. Because draw-tower gratings are inscribed by a single pulse, this requirement is automatically fulfilled and, in addition, there is no decoating and recoating problem.

5. Thermal Characterization

In section 1, we described an FBG as a "permanent" periodic structure; yet, the degree of permanence has to be adequately investigated. Photosensitivity theory states that carriers (e.g. electrons) are excited by UV excitation and then trapped into a continuous distribution of energy states, rather than at a single trap level due to the amorphous structure of the germanium-doped silicate glass [23]. As a consequence, the process can be inverted by thermal excitation. The detrapping from any state is assumed to be dependent on the excitation energy and the depth of each state. After the detrapping process, the electrons presumably occupy the same states as before UV excitation, i.e. the UV-induced index changes and, thus, the grating disappears.

The pertinent questions are at which temperature the decay process starts and how long the decay process takes. It has been shown that the thermal stability of FBGs depends on the same parameters as the UV-induced change in the refractive index [6]. This means the thermal stability is a function of the fiber material, the fabrication technique, and the treatment of the fiber before UV illumination.

As noted above, for the use in sensor applications, high demands are placed on the reliability of the FBGs and, therefore, special interest focuses on the thermal stability of on-line fabricated gratings [24]. For the thermal characterization of FBGs, the gratings were heated to elevated temperatures in a furnace. The grating reflectivity was measured as a function of time. But instead of grating reflectivity, the normalized integrated coupling constant (ICC) was chosen as a measure of the grating strength. This quantity is proportional to the UV-induced change in the refractive index, even in the case of a nonuniform grating. The normalized ICC is defined as follows:

$$\textit{normalized ICC} = \frac{\tanh^{-1}\left(\sqrt{R(t)}\right)}{\tanh^{-1}\left(\sqrt{R_0}\right)} \qquad (4)$$

with R(t) the time-dependent grating reflectivity and R_0 the grating reflectivity at t = 0.

Because of the low reflectivity (<5%) and the small full-width at half-maximum (FWHM, ~100 pm at 1.5 µm) of the on-line fabricated gratings, special requirements are set for the measurement technique. We have developed a measurement set-up which consists of a tunable laser source, e.g. an external cavity laser, and an additional wavelength attachment unit to allow high-accuracy wavelength and reflectivity detection [13].

We studied the thermal decay of six on-line fabricated gratings which were provided by the IPHT in Jena, Germany. The grating reflectivities at t = 0 were in the range of 0.8 – 1.9 %. We observed a high polarization dependency of the gratings of up to 30 % of the initial reflectivity, which produces some uncertainties in the determination of the normalized ICC. In the decay experiments, FBGs were heated in pairs at temperatures of 150 C, 250 C, and 350 C. We decoated the gratings before they were put in the furnace. Then we measured the grating reflectivity as a function of time at constant temperature. Data was then combined and plotted in the curves shown in Figures 6, 7, and 8. The high scattering of data at a fixed time is caused by the large polarization dependency. As can be seen from Figures 6, 7, and 8, the UV-induced change in the refractive index initially decays very rapidly, but the rate of decay decreases as time advances. After a certain time, the normalized ICC reaches a limit. The decay also strongly depends on the temperature. We obtained a decay of approx. 60 % of the gratings exposed to a temperature of 150 C and a decay of approx. 98 % of the gratings exposed to a temperature of 350 C. For the latter, this means that, of an initial reflectivity of 1 %, a reflectivity of 0.02 % remains at 350 C. However, the grating sensor can still be used if this very low-reflective grating can be resolved by means of an appropriate measurement technique.

Lifetime predictions based on the results of our experiments are not possible for reasons of the low number of gratings investigated and the strong scattering of individual data points. However, it seems to be possible to overcome the current limitations in the thermal stability by the use of appropriate fibers. Hence, we can state that using the on-line fabricated fibers provided to us in a temperature-range relevant to aerospace applications (up to 100 C), the thermal stability of the gratings can be warranted over decades.

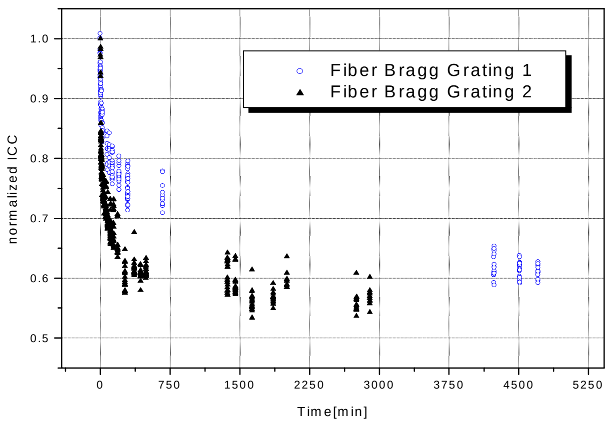

Figure 6: Thermal Decay of FBGs at T = 150° C

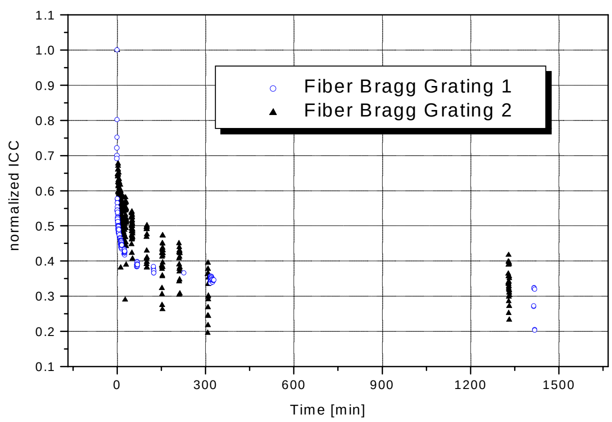

Figure 7: Thermal Decay of FBGs at T = 250° C

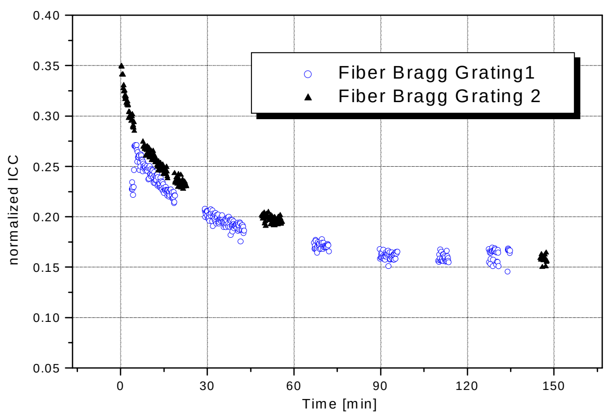

Figure 8: Thermal Decay of FBGs at T = 350° C

6. Results from a Field Test at DASA Airbus

At the DaimlerChrysler Aerospace Airbus test center in Hamburg, the fatigue performance of a newly developed wing consisting of a carbon fiber-reinforced plastics (CFRP) was examined from September 1998 to December 1999. This kind of structure diagnosis makes it necessary to deploy a large number of electrical strain gauges, in particular for flight test installations. Typically, a single resistive strain gauge needs four connecting wires and, in our concrete case, the wing was paved with about 800 electrical strain gauges. The technique is time consuming and, therefore, extremely expensive. Using the excellent multiplexing capabilities of Bragg grating sensors, a significant cost reduction can be expected under the assumption that the price per sensor can be reduced even further in the next few years. To demonstrate and test the new technique, two arrays, each consisting of 11 Bragg grating sensors, were glued to the surface of the wing using our patented mounting technique. All the sensors were placed right next to existing electrical strain gauges and strain rosettes. Half of the sensors were mounted on the lower skin and the other half on the upper skin of the CFRP wing. In these initial investigations, no special care was taken to protect the sensors. Two sensors from each array were used only as temperature sensors. With the help of these sensors, the influence of the temperature on the other sensors was corrected. The sensor interrogation was carried out with the measurement system mentioned in section 5.

One array was fabricated with a phase mask method used by a commercial supplier. Typical grating parameters are 6.5 mm for the grating length, a reflectivity of 7 % and a FWHM of 110 pm. We used a polyimide-coated fiber with a polyimide recoating in the grating region. The intrinsic polarization dependence of the Bragg resonance (as a mean value) was found to be $|\lambda_{Bp}-\lambda_{Bq}|\approx 6$ pm unstrained and at constant temperature. The other array was fabricated online at the draw-tower by the IPHT in Jena (Germany). Typical grating parameters are 5.5 mm for the grating length, a reflectivity of 1.3 % and a FWHM of 130 pm. Again the fiber was polyimide coated and no recoating was needed. The intrinsic polarization dependence of the Bragg resonance (as a mean value) was found to be $|\lambda_{Bp}-\lambda_{Bq}|\approx 5$ pm unstrained and at constant temperature.

In Table 2, the measurement results for a selected sensor are shown for a period of time of one year. During the year, the wing was heated with water to accelerate the fatigue, which explains the different surface temperatures. In addition, it was continuously loaded to simulate the complete lifetime of a passenger aircraft. In June, 60,000 “flights” were carried out with the wing. This corresponds to one aircraft operational life. During this time, the sensors were subjected to approximately 12 million load points. Maximum strain levels (overload case) at the position of the FBG sensors were ± 3000 µm/m. As Table 1 shows, the consistency between the values of the electrical strain gauge and the FBG sensor was found to be excellent for each load level during one measurement. Also, the reproducibility of the measurements over the whole year is staggering. All of the data was obtained using Equation 5 with calibration constants ascertained before mounting the sensors to the wing. Similar results have been obtained for most of the other sensors.

During the mounting of the sensors, only one sensor was lost, apparently due to a poor recoating. During the year of measurements, four more sensors were lost from the bottom shell, mainly because the glued sensor location was in contact with water running over the wing. This led to the glue and the fiber coating detaching from the wing, which is also a problem for electrical strain gauges. A further concern was the unprotected fiber line between the sensors. Oftentimes people working on the wing were not able to see the fiber. Sometimes a fiber fracture was the result. Of course this was easily repaired by splicing the fiber. However it may become critical if the fiber fracture occurs near a sensor.

	September 1998 Load Case (LC) 031 $T_{surface}$=22 °C		March 1999 LC similar to 031 $T_{surface}$=39 °C		June 1999 LC 031 $T_{surface}$=50 °C		December 1999 LC 031 $T_{surface}$=53 °C	
Load level j	**Reference [µm/m]**	**FBGS [µm/m]**	**Reference [µm/m]**	**FBGS [µm/m]**	**Reference [µm/m]**	**FBGS [µm/m]**	**Reference [µm/m]**	**FBGS [µm/m]**
0	0	0	0	-0,1	2	0	2	0
0.2	-263	-259.6	-259	-251.7	-255	-259.9	-282	-284.3
0.4	-526	-519.0	-519	-516	-530	-529.9	-546	-548.4
0.6	-791	-782.3	-785	-781.2	-797	-792.6	-811	-810.8
0.8	-1059	-1047.2	-1035	-1032.6	-1056	-1047.8	-1075	-1077.5
0.9	-1192	-1178.8	-1170	-1168.9	--	--	--	--
1	-1326	-1310.1	-1309	-1300.4	-1330	-1316.3	-1345	-1341.5
0.8	-1061	-1049.0	-1041	-1038.2	-1059	-1062.1	--	--
0.4	-532	-527.0	-526	-524.6	-514	-525.7	--	--
0	-2	0.2	0	-0.7	13	-0.6	--	--

Table 2: Example of Measured Data at One Position on the Wing. Reference Is the Nearest Electrical Strain Gauge.

As a result, accurate and practical methods for the protection of the sensors and the fiber are currently being developed. In particular, this will become vital in hasher environments, e.g. in flight tests. In addition, the temperature compensation method used in this experiment only works well because the temperature changes were small (± 1 C) and relatively homogenous during a measurement, leading to small strain errors even if the temperature at the sensor location was not known exactly. In a flight test, the temperature changes are much larger and relatively rapid. In such an application, the temperature must be known with a higher spatial resolution than in the previous experiment. Of course this can be achieved using a temperature sensor at each strain sensor location, but sensing strain and temperature with the same sensor and distinguishing between both effects would be much more practical. There is a variety of solutions to this problem [e.g. 13, 15].

6. Summary

We discussed various aspects of the grating fabrication process and the fiber coating concerning the use of fiberoptic Bragg gratings as strain sensors in future avionics systems. The mechanical strength of FBGs is a function of properties of the coating material and parameters of the fabrication process. Although there have been some reports of UV-transparent coatings, so far, the best solution to the mechanical problem, taking cost considerations into account, seems to be the direct fabrication of Bragg gratings on the draw-tower. Our results on the thermal stability of draw-tower gratings show the suitability of these sensors within the temperature range relevant to aerospace applications. The results of a field test performed at DASA Airbus clearly show the functionality of the fiberoptic sensor system based on Bragg gratings.

Acknowledgements

We thank the Institute of Physical High Technology e.V. IPHT, Modern Optics Division, Jena (Germany), for fabricating the FBGS online and for useful discussion. We thank the Technical University of Dresden, High Frequency Department, Dresden (Germany), for preparing the off-line fabricated FBGS.
We thank Prof. Dr. Klaus Petermann, Technical University of Berlin, High Frequency Department, Berlin (Germany), for useful discussion.

References

[1] W. Martin et al. Advances in Adaptive System Applications at Daimler-Benz Research Labs. *International Mechanical Engineering Congress; Dallas (USA) Nov. 1997*, Adaptive Structures and Materials Systems Book No. H01103-11997

[2] C. Bauer, W. Martin, H.-F. Siegling. An adaptive composite structure to control the sonic shock of transport aircraft wings. *Proceedings; Smart Structure and Materials; 25-32; Harrogate (U.K.)* 6-8 July 1998

[3] Othonos A, Kalli K. *Fiber Bragg Gratings Fundamentals and Applications in Telecommunication and Sensing.* Artech House, Boston, 1999

[4] M. Trutzel, H.-F. Siegling, D. Betz, R. Sangkohl, M. Holz, L. Staudigel, W. Martin, O. Krumpholz. Determination of Strain and Temperature Fields using Fiberoptic Bragg Grating Sensors. Sensor'99; May 20, 1999, Nuremberg (Germany)

[5] T. Wei, H.H. Yuee, C.H. Hasz, P.L. Key. Degradation of fiber strength during coating stripping; *International Wire & Cable Symposium Proceedings*; pp. 199-204; 1989

[6] T. Volotinen, W. Griffioen, M. Gadonna, H. Limberger. *Reliability of Optical Fibers and Components Final Report of COST 246*, Springer Verlag, 1999

[7] L. Dong, J.-L. Archambault. L. Reekie, P.St.J. Russell and D.N. Payne. Single pulse Bragg gratings written during fiber drawing. *Electronics Letters*, 29, pp. 1577-1578, 1993

[8] C.G. Askins, M.A. Putnam, G.M. Williams and E.J. Friebele. Stepped-wavelength optical fiber Bragg grating arrays fabricated in line on a draw tower. *Optics Letters*, 19, pp. 147-149, 1994

[9] Hagemann, V.; Rothhardt, M.; Mueller, H.-R; Trutzel, M.N.; Staudigel, L.; Krumpholz, O., "Mechanical resistance of draw-tower-Bragg-grating sensors"; *Electronics Letters*, Vol. 34, No. 2, pp. 211-212, 1998

[10] Internet Reference. http://www-nesb.larc.nasa.gov/people/x33.html.

[11] L. Chao, L. Reekie, M. Ibsen. Grating writing through fiber coating at 244 and 248nm. *Electronics Letters*, 35, No.11, pp 924-926, 1999

[12] Ph. M. Nellen, A. Frank, P. Mauron, U. Sennhauser. Lifetime and reliability of embedded optical sensor fibers. *International Workshop on Fiber Optic Sensors for Construction Materials and Bridges.* Newark, NJ, USA, May 3-6, 1998

[13] Trutzel, M.N.; Wauer, K.; Betz, D.; Staudigel, L.; Krumpholz, O.; Muehlmann, H.C.; Muellert, T.; Gleine, W. Smart Sensing of Aviation Structures with Fiber-optic Bragg Grating Sensors. *Smart Structures and Materials 2000: Sensory Phenomena and Measurement Instrumentation for Smart Structures and Materials, Newport Beach, USA, March 2000*

[14] Trutzel, M.N.; Kibler, T.; Betz, D.; Wauer, K.; Staudigel, L.; Krumpholz, O.; Siegling, H.-F.; Sangkohl, R.; Martin, W. Sensorverhalten werkstoffintegrierter Bragg-Gitter-Sensoren. *Sensoren und Messsysteme 2000*, March 13-14 2000, Ludwigsburg (Germany)

[15] [Trutzel, M.N.; Betz, D.; Holz, M.; Staudigel, L.; Krumpholz, O.; Siegling, H.F.; Sangkohl, R.; Martin, W.; Muehlmann, H.C.; Muellert, T.; Ahrendt, H. Investigation of Fiberoptic Bragg Grating Sensors for Applications in the Aviation Industry. *in 13th International Conference on Optical Fiber Sensors, Proceedings of SPIE Vol. 3746*, pp. 624-627 ,1999

[16] D.R. Biswas. *Fiber Optics Reliability and Testing, Critical Reviews of Optical Science and Technology / Ed. D.K. Paul – Bellingham*, Wash.: SPIE 1994, Optical Fiber Coatings (pp 63-79).

[17] D.K. Nath, G.W. Nelson, S.E. Griffin, C.T. Harrington. Polyimide coated embedded optical fiber sensors. *SPIE Vol. 1489*, pp.17-32, 1991

[18] R.W. Cahn (Ed.). Materials science and technology Vol. 9, Glasses and amorphous materials. VCH-Verlag, 1991

[19] D. Varelas, D.M. Costantini, H.G. Limberger, R.P. Salathé. Fabrication of high-mechanical-resistance Bragg gratings in single-mode optical fibers with continuous-wave ultraviolet laser side exposure. *Optics Letters*, 23, No. 5, 397, 1998

[20] D. Varelas, H.G. Limberger, R.P. Salathé, C. Kotrotsios. UV-induced mechanical degradation of optical fibres. *Electronics Letters*, 33, pp. 804-806, 1997

[21] International Electrotechnical Commission IEC; International Standard (CEI-IEC 793-1-3); Optical fibers, 1995

[22] F.P. Kapron, H.H. Yuce. Theory and measurement for predicting stressed fiber lifetime. *Optical Engineering*, Vol. 30, No. 6, 1991

[23] Erdogan, T.; Mizrahi, V.; Lemaire, P.J.; Monroe, D. Decay of ultraviolet-induced fiber Bragg gratings. *Journal of Appl. Physics.*, Vol. 76, No. 1, 73-80, 1994

[24] Mauron, P.; Nellen, Ph.M.; Sennhauser, U.; Trutzel, M.N.; Betz, D.; Hagemann, V.; Rothardt, M. Lifetime of Fibre Bragg Gratings Under Cyclic Fatigue. *SPIE's International Symposium on Voice, Video and Data Communications, Program on Optical Fiber Devices and Systems, VV12: Conference on Optical Fiber reliability and Testing*, Boston, 1999